Title

AKR1C3 Promotes AR-V7 Protein Stabilization and Confers Resistance to AR-Targeted Therapies in Advanced Prostate Cancer

Journal

Molecular Cancer Therapeutics, 18(10)

ISSN

1535-7163

Authors

Liu, Chengfei
Yang, Joy C
Armstrong, Cameron M
et al.

Publication Date

2019-10-01

DOI

10.1158/1535-7163.mct-18-1322

Peer reviewed

HHS Public Access

Author manuscript

Mol Cancer Ther. Author manuscript; available in PMC 2020 April 01.

Published in final edited form as:

Mol Cancer Ther. 2019 October ; 18(10): 1875–1886. doi:10.1158/1535-7163.MCT-18-1322.

AKR1C3 promotes AR-V7 protein stabilization and confers resistance to AR-targeted therapies in advanced prostate cancer

Chengfei Liu[1], **Joy C. Yang**[1], **Cameron M. Armstrong**[1], **Wei Lou**[1], **Liangren Liu**[1], **Xiaomin Qiu**[1], **Binhao Zou**[1], **Alan P. Lombard**[1], **Leandro S D'Abronzo**[1], **Christopher P. Evans**[1,2], **Allen C. Gao**[1,2,3,*]

[1]Department of Urologic Surgery, University of California Davis, CA;

[2]UC Davis Comprehensive Cancer Center, University of California Davis, CA;

[3]VA Northern California Health Care System, Sacramento, CA;

Abstract

The mechanisms resulting in resistance to next generation anti-androgens in castration resistant prostate cancer are incompletely understood. Numerous studies have determined that constitutively active androgen receptor (AR) signaling or full length AR bypass mechanisms may contribute to the resistance. Previous studies established that AKR1C3 and AR-V7 play important roles in enzalutamide and abiraterone resistance. In the present study, we found that AKR1C3 increases AR-V7 expression in resistant prostate cancer cells through enhancing protein stability via activation of the ubiquitin mediated proteasome pathway. AKR1C3 reprograms AR signaling in enzalutamide resistant prostate cancer cells. Additionally, bioinformatical analysis of indomethacin treated resistant cells revealed that indomethacin significantly activates the unfolded protein response (UPR), p53 and apoptosis pathways, and suppresses cell cycle, Myc and AR/ARV7 pathways. Targeting AKR1C3 with indomethacin significantly decreases AR/AR-V7 protein expression in vitro and in vivo through activation of the ubiquitin mediated proteasome pathway. Our results suggest that the AKR1C3/AR-V7 complex collaboratively confers resistance to AR targeted therapies in advanced prostate cancer.

Keywords

Prostate cancer; AKR1C3; AR-V7; resistance

Introduction

Recently approved androgen receptor signaling inhibitors (ARSI) such as enzalutamide, abiraterone and apalutamide improved the therapeutics for advance prostate cancer including castration resistant prostate cancer (CRPC) patients (1–3). These ARSIs surpass the effect of conventional androgen deprived therapy (ADT) using GnRH receptor agonists and

*To whom correspondence should be addressed: acgao@ucdavis.edu, Mailing address: Research III Bldg, Suite 1300, 4645 2nd Ave, Sacramento, CA 95817, Phone: 916-734-8718.

Conflicts of Interest: All authors have no conflicts of interest.

antagonists to circumvent androgen production to aid tumor progression (4). However, drug resistance still emerges with amplification of AR variants as the leading cause for the escape mechanism. Constitutively active AR variants can activate distinct transcriptional program and confers enzalutamide and abiraterone resistance (5–7). AR variants can be generated either by gene rearrangement or mRNA splicing (8–10). However, regulation of AR variants at the protein level is still incompletely understood.

Previous studies demonstrate that AKR1C3 promotes enzalutamide and abiraterone resistance by activating the androgen biosynthesis pathway and AR signaling (11, 12). AKR1C3, also called HSD17B5, is a critical gene in androgen synthesis. Upregulation of AKR1C3 was readily observed in abiraterone and enzalutamide resistant prostate cancer cells. Not only does this play a central role in intracrine androgen biosynthesis; its expression is also closely correlated to disease stage (13–15). Moreover, intracrine steroids, including androgens, were elevated in castration and ARSI resistant cells, which could be due to overexpression of steroidogenic genes such as AKR1C3 (11, 16, 17). AKR1C3 binds with full-length AR and co-activates AR in prostate cancer cells (18). In addition to the enzyme activity of AKR1C3, other functions of AKR1C3 haven’t been fully investigated yet.

In this study, we demonstrate that AKR1C3 reprograms AR/AR-V7 signaling in enzalutamide resistant cells. AKR1C3 induces AR-V7 overexpression and stabilizes AR-V7 protein in resistant cells through alteration of the ubiquitin proteasome system. Targeting AKR1C3 by indomethacin activates UPR and p53 pathways but suppresses AR/AR-V7 signaling. Orally administrated indomethacin significantly enhances enzalutamide treatment through AKR1C3/AR-V7 signaling suppression. Our results highlight the role of AKR1C3/AR-V7 complex in enzalutamide and abiraterone resistance.

Materials and Methods

Cells lines and tissue culture

LNCaP, C4–2B and CWR22Rv1 were maintained in RPMI1640 supplemented with 10% fetal bovine serum (FBS), 100 units/ml penicillin and 0.1 mg/ml streptomycin. 293 cells were maintained in DMEM supplemented with 10% fetal bovine serum (FBS), 100 units/ml penicillin and 0.1 mg/ml streptomycin. All experiments with cell lines were performed within 6 months of receipt from the ATCC or resuscitation from cryopreservation. C4–2B cells were kindly provided and authenticated by Dr. Leland Chung, Cedars-Sinai Medical Center (Los Angeles, CA). The resistant cells were developed and are referred to as C4–2B MDVR (C4–2B enzalutamide resistant) and C4–2B AbiR (C4–2B abiraterone resistant) as previously described (19). C4–2B MDVR and C4–2B AbiR cells were maintained in 20 μM enzalutamide containing medium and 10 μM abiraterone acetate containing medium respectively. Parental C4–2B cells were passaged alongside the resistant cells as an appropriate control. All cells were maintained at 37°C in a humidified incubator with 5% carbon dioxide. Enzalutamide, abiraterone acetate, and indomethacin were purchased from Selleck Chemicals.

Plasmids and cell transfection

For transfection of small interfering RNA (siRNA), cells were seeded at a density of 0.5×10^5 cells per well in 12-well plates or 2×10^5 cells per well in 6-well plates and transfected with 20nM of siRNA targeting the AR-V7 sequence (GUAGUUGUGAGUAUCAUGA) or control siRNA (Catalog# 12935300) using Lipofectamine-iMAX (Invitrogen). The effect of siRNA-mediated gene silencing was examined using qRT-PCR and western blot 2–3 days after transfection. Lentiviral plasmids encoding shRNA targeting AKR1C3 (TRCN0000026561) were purchased from Sigma-Aldrich. pLenti-GFP Lentiviral control vector were used as control. Lentiviral particles were produced in 293T cells after co-transfection of the lentivirus vectors, psPAX2 and pMD2.G in 10-cm dishes. The lentivirus containing medium was collected and cells were infected.

Protein extraction and western blotting

Whole cell protein extracts were resolved on SDS-PAGE and proteins were transferred to nitrocellulose membranes. After blocking for 1 hour at room temperature in 5% milk in PBS/0.1% Tween-20, membranes were incubated overnight at 4oC with the indicated primary antibodies AR (441), AR (N-20), Ubiquitin (P4D1 and FL76), 1:1000 dilution, Santa Cruz Biotechnology, Santa Cruz, CA. AR-V7 (AG10008, Mouse monoclonal antibody, 1:1000 dilution, precision antibody); FLAG® M2 monoclonal antibody (F1804, 1:1000 dilution, Sigma-Aldrich, St. Louis, MO); AKR1C3 (A6229, 1:1000 dilution, Sigma-Aldrich, St. Louis, MO); AKR1C3 (11194–1-AP, 1:1000 dilution, Proteintech Group, Inc); Tubulin (T5168, Monoclonal Anti-α-Tubulin antibody, 1:5000 dilution, Sigma-Aldrich, St. Louis, MO). Tubulin was used as loading control. Following secondary antibody incubation, immunoreactive proteins were visualized with an enhanced chemiluminescence detection system (Millipore, Billerica, MA).

Cell growth and survival assay

LNCaP-neo or LNCaP-AKR1C3 cells were seeded on 12-well plates at a density of 0.3×10^5 cells/well in phenol red free RPMI 1640 media containing 10% CS-FBS. Total cell number was determined at 0, 3 and 5 days. LNCaP-AKR1C3 or C4–2B-AKR1C3 cells were transiently transfected with siRNA targeting AR-V7 or a control siRNA, and then treated with enzalutamide for 3 days and total cell number was counted.

Real-Time quantitative RT-PCR

Total RNA was extracted using TriZOL reagent (Invitrogen). cDNA was prepared after digestion with RNase-free RQ1 DNase (Promega) and then subjected to real-time reverse transcription-PCR (RT-PCR) using Sso Fast Eva Green Supermix (Bio-Rad) according to the manufacturer's instructions and as described previously (20). Each reaction was normalized by co-amplification of actin. Triplicates of samples were run on default settings of a Bio-Rad CFX-96 real-time cycler. The primer sequences are Primers used for RT-PCR were: AR-full length: Forward (F)-AAG CCA GAG CTG TGC AGA TGA, Reverse (R)-TGT CCT GCA GCC ACT GGT TC; AR-V7: F-AAC AGA AGT ACC TGT GCG CC, R-TCA GGG TCT GGT CAT TTT GA; KLK3: F-GCC CTG CCC GAA AGG, R-GAT CCA CTT CCG GTA ATG CA; FKBP5: F-AGA ACC AAA CGG AAA GGA GA, R-GCC ACA TCT CTG CAG

TCA AA; UBE2C: F-TGG TCT GCC CTG TAT GAT GT, R-AAA AGC TGT GGG GTT TTT CC; Myc: F-TGA GGA GAC ACC GCC CAC, R-CAA CAT CGA TTT CTT CCT CAT C; FHL2: F-ACC AAG AGT TTC ATC CCC, R-TCA GGC AGT AGG CAA AGT; MED12: F-CTG GAC GAA GAT CGC GTC TG, 3-ATT CAA GCA GCT ATG GGA TTC AA; FKBP4: 5-GTC ATC AAG GCT TGG GAC AT, 3-CCC TCA TTG GGC TTA GCA TA; NCOA3: 5-GGT AGG CGG CAT GAG TAT GTC, 3-TGT TAC TGG AAC CCC CAT ACC T; Actin: F-AGA ACT GGC CCT TCT TGG AGG, R-GTT TTT ATG TTC CTC TAT GGG.

Co-immunoprecipitation assay

Equal amounts of cell lysates (1500 μg) were immunoprecipitated using 1 μg of AKR1C3 antibody with 50 μL of protein A/G agarose with constant rotation overnight. The immunoprecipitants were washed with 10 mM HEPES (pH 7.9), 1 mM EDTA, 150 mM NaCl, and 1% Nonidet P-40 twice with 1 mL each. The precipitated proteins were eluted with 30 μL of SDS-PAGE sample buffer by boiling for 10 minutes. The eluted proteins were electrophoresed on 8% SDS-PAGE, transferred to nitrocellulose membranes, and probed with indicated antibodies.

RNA-seq data analysis

C4–2B MDVR cells were treated with vehicle or the AKR1C3 inhibitor indomethacin for 24 h before RNA extraction. RNA-seq libraries from 1 μg total RNA were prepared using Illumina Tru-Seq RNA Sample, according to the manufacturer's instructions. mRNA-Seq paired-end library was prepared through Illumina NGS on HiSeq 4000: 2 ×150 cycles/bases (150bp, PE). Around 30M reads/sample were generated. Data analysis was performed with a Top Hat-Cufflinks pipeline and sequence read mapping/alignment using HISAT. StringTie Data was mapped to and quantified for 60,658 unique genes/transcripts Gene and transcript expression is quantified as FPKM (Fragments Per Kilobase of transcript per Million mapped reads). Principal Component Analysis (PCA) was conducted on the FPKM gene-level data for all genes/transcripts passing filter (Filtered on Expression > 0.1) in the Raw Data. The genes regulated by indomethacin treatment were clustered with Hierarchical Clustering algorithm by StrandNGS software. The RNA sequence data in the present study have been deposited in Gene Expression Omnibus (GEO) with the accession number GSE129596.

Gene Set Enrichment Analysis (GSEA)

GSEA was performed using the Java desktop software (http://software.broadinstitute.org/gsea/index.jsp), as described previously (21). Genes were ranked according to the shrunken limma $\log^2$ fold changes, and the GSEA tool was used in 'pre-ranked' mode with all default parameters. KEGG-Ubiquitin mediated proteolysis pathway was used in the GSEA analysis.

Dual immunofluorescence assay

1×10^4 293 cells were plated in 4-well Nunc™ Lab-Tek™ II Chamber Slides and transfected with AR-V7, AKR1C3 for 3 days. Cells were fixed with 4% paraformaldehyde, permeabilized with 0.5% Triton X-100, and incubated with 1% BSA to block nonspecific binding. Cells were incubated with anti-AR (N20, Santa Cruz Biotechnology) and anti-

AKR1C3 antibodies (A6229, Sigma-Aldrich, St. Louis, MO) overnight. Intracellular AR-V7 was visualized with FITC-conjugated secondary antibodies, AKR1C3 was visualized with Texas red conjugated secondary antibodies and nuclei were visualized with DAPI by All-in-One Fluorescence Microscope (BZ-X700).

Animal studies and treatment regimens

All experimental procedures using animals were approved by the Institutional Animal Care and Use Committee of UC Davis. CWR22Rv1 cells (4 million) were mixed with matrigel (1:1) and injected subcutaneously into the flanks of 5–6 week old male SCID mice. Tumor-bearing mice (tumor volume around 50–100 mm^3) were randomized into six groups (6 mice per group) and treated as follows: (1) vehicle control (15% Cremophor EL, 82.5% PBS and 2.5% dimethyl sulfoxide (DMSO), i.p.), (2) enzalutamide (25 mg/kg, p.o.), (3) Indomethacin (3 mg/kg, p.o.), or (4) enzalutamide (25 mg/kg, p.o.) + Indomethacin (3 mg/kg, p.o.). Tumors were measured using calipers twice a week and tumor volumes were calculated using length × $width^2/2$. Tumor tissues were harvested and weighed after 3 weeks of treatment.

To assess the effect of enzalutamide on the growth of LNCaP-AKR1C3 tumors, 3–4 week old SCID C.B17 mice were orthotopically injected with 2 million LNCaP-AKR1C3 cells into the prostate. After the mice plasma PSA reached to 5–10 ng/mL, the mice were surgically castrated. Two weeks later, the mice were randomized into two groups (4 mice per group) and treated as follows: (1) vehicle control (15% Cremophor EL, 82.5% PBS and 2.5% dimethyl sulfoxide (DMSO), i.p.), (2) enzalutamide (20 mg/kg, p.o.). Mice PSA level was monitored every week. Tumor tissues were harvested and weighed after 4 weeks of treatment.

Sample preparation and steroid analysis

The steroid extraction and analysis has been described previously (11, 22). Briefly, tumor samples (eight each of C4–2B tumors and MDVR tumors) were ground and suspended in 4 mL of a 1:1 water/methanol mixture. The suspension was homogenized, and the resulting homogenate was cooled on ice. The precipitated material was removed by centrifuging at high speed for 5 min, and the supernatant was removed and evaporated in a SpeedVaac (Labconco Inc.) followed by lyophilizer (Labconco Inc.). The residue was suspended in 150 μL of CH3OH/H2O (1:1), filtered through a 0.2 μm ultracentrifuge filter (Millipore inc.) and subjected to UPLC/MS-MS analysis. Samples were run in duplicate during UPLC-MS/MS analysis. Samples were placed in an Acquity sample manager which was cooled to 8 °C to preserve the analytes. Pure standards were used to optimize the UPLC-MS/MS conditions prior to sample analysis. The standard mixture was run before the first sample to prevent errors due to matrix effect and day-to-day instrument variations. In addition, immediately after the initial standard and before the first sample, two spiked samples were run to calibrate for the drift in the retention time of all analytes due to the matrix effect. After standard and spiked sample runs, a blank was injected to wash the injector and remove carry over effect.

Immunohistochemistry

Tumors were fixed by formalin and paraffin embedded tissue blocks were dewaxed, rehydrated, and blocked for endogenous peroxidase activity. Antigen retrieval was performed in sodium citrate buffer (0.01 mol/L, pH 6.0) in a microwave oven at 1,000 W for 3 min and then at 100 W for 20 min. Nonspecific antibody binding was blocked by incubation with 10% fetal bovine serum in PBS for 30 min at room temperature. Slides were then incubated with anti-AR (N20, at 1:200; Santa Cruz Biotechnology) at 4°C overnight. Slides were subsequently washed and incubated with biotin-conjugated secondary antibodies for 30 min, followed by incubation with avidin DH-biotinylated horseradish peroxidase complex for 30 min (Vectastain ABC Elite Kit, Vector Laboratories). The sections were developed with the diaminobenzidine substrate kit (Vector Laboratories) and counterstained with hematoxylin. Nuclear staining of cells was scored and counted in 5 different vision fields. Images were taken with an Olympus BX51 microscope equipped with DP72 camera.

Statistical Analysis

All data are presented as means ± standard deviation of the mean (SD) from three independent experiments. Statistical analyses were performed with SPSS16.0. Differences between individual groups were analyzed by two tailed student's t test or one-way analysis of variance (ANOVA) followed by the Scheffé procedure for comparison of means. $p<0.05$ was considered statistically significant.

Results

The steroid hormone biosynthesis pathway is activated and AR/AR-V7 signaling is distinctly regulated in enzalutamide resistant cells

It is crucial to understand how prostate cancer evolves to the drug resistant stage and identify early intervention strategies for treating CRPC patients. Towards this goal, we have developed enzalutamide resistant C4–2B MDVR cells (11). To understand potential resistance mechanisms, RNA sequence data from the C4–2B MDVR and parental cells were analyzed. As shown in Fig.1A, a significant enrichment of steroid hormone biosynthesis signaling was revealed in C4–2B MDVR cells ($p<0.05$) as well as in mouse LNCaP/AR xenograft tumors derived from enzalutamide resistant LREX' cells ($p<0.001$) (23) by the Gene Sets Enrichment Analysis (GSEA). Data analysis showed that genes such as AKR1C3 involved in androgen biosynthesis were upregulated in the enzalutamide-resistant xenograft tumors (Fig.1B and Supplemental Fig.1). Classically, AKR1C3 is one of the most important enzymes catalyzing androstenedione conversion to testosterone, and it also facilitates the 5' dione and back door synthesis pathways by catalyzing 5α' androstenedione and androsterone to 5' androstanediol, respectively. Both products are then converted to Dihydrotestosterone (DHT). Our previous study showed that C4–2B MDVR cells had significantly higher androgen production compared to the parental line (11). In the present study, we confirmed these results in xenograft tumors by LC-MS. As shown in Fig.1C, C4–2B MDVR xenograft tumors expressed significantly higher testosterone levels compared to C4–2B parental xenograft tumors ($p=0.0301$). IHC staining of AR in C4–2B MDVR xenografts was predominately in the nucleus compared to C4–2B parental tumors (Fig.1D). To examine the AR response to androgen stimulation, C4–2B parental or C4–2B MDVR

cells were cultured in Charcoal Stripped Fetal Bovine Serum (CS-FBS) conditions for 3 days and treated with 10nM DHT overnight. As shown in Fig.1E, C4–2B MDVR cells expressed significantly higher AR levels by DHT stimulation compared to C4–2B parental cells. Levels of AR-V7, AKR1C3 and c-Myc were upregulated in C4–2B MDVR cells. To further determine the AR/AR-V7 signaling pathway regulation in enzalutamide resistance cells, expression of genes involved in androgen receptor signaling was analyzed. As shown in Fig.1F–1G, the expression of several AR/AR-V7 co-activators were significantly up regulated in C4–2B MDVR cells, such as FHL2, MED12, FKBP4 and NCOA3; but that of classical AR target genes, such as PSA was decreased (Supplemental Fig.2), which suggested a distinct AR signaling is constitutively active in C4–2B MDVR cells. Taken together, the results showed that steroid hormone biosynthesis pathway and a distinct AR signaling are activated in resistant C4–2B MDVR cells.

AKR1C3 binds with AR-V7 and induces AR/AR-V7 protein overexpression

Our previous study found knockdown of AKR1C3 downregulated AR and AR-V7 expression in resistant cells (12). To understand how AKR1C3 regulates AR/AR-V7 expression, we constructed stable AKR1C3 overexpressing LNCaP and C4–2B cells and determined AR/AR-V7 expression. As shown in Fig.2A and Supplemental Fig.3, AKR1C3 overexpressing LNCaP-AKR1C3 and C4–2B-AKR1C3 cells express higher levels of AR-V7 and AR-FL protein compared to LNCaP-neo and C4–2B-neo cells. Other AR variants were also increased by the pan-AR antibody determination; however, AKR1C3 overexpression did not affect AR-FL or AR-V7 mRNA levels in either LNCaP-AKR1C3 or C4–2B-AKR1C3 cells (Fig.2B). Next, we determined if AKR1C3 binds with AR-V7 in resistant cells. As shown in Fig.2C, AKR1C3 and AR-V7 formed complex in both C4–2B MDVR and CWR22Rv1 cells. The results were also confirmed by dual immunofluorescence staining (Fig.2D).

To further investigate the role of AKR1C3 in castration resistance, we first determined that overexpression of AKR1C3 significantly promoted the LNCaP cell growth in CS-FBS condition (Fig.3A). Then we used an *in vivo* xenograft model to determine the effects of enzalutamide in the LNCaP-AKR1C3 stable cell line. As shown in Fig.3B–3C, LNCaP-AKR1C3 cells slightly responded to the castration; within 1–2 weeks, the tumors were starting to relapse and the relapsed LNCaP-AKR1C3 tumors were resistant to enzalutamide treatment. We also determined the AR-V7 level in LNCaP-AKR1C3 tumors. As shown in Fig.3D, LNCaP-AKR1C3 tumors expressed significantly higher AR-V7 compared to the LNCaP-neo cells. To further determine if AKR1C3 induced AR-V7 overexpression confers resistance to enzalutamide, AR-V7 was knocked down in LNCaP-neo and LNCaP-AKR1C3 cells and then treated with enzalutamide. Knockdown of AR-V7 slightly reduced growth of LNCaP-neo cells but enzalutamide itself significantly suppressed their growth. Knockdown of AR-V7 in combination with enzalutamide did not further reduce cell growth, indicating that AR-V7 knockdown had no effect on the sensitivity of LNCaP-neo cells to enzalutamide (Supplemental Fig.4). In LNCaP-AKR1C3 cells with higher levels of AR-V7, knockdown of AR-V7 slightly decreased cell proliferation; however, AR-V7 knockdown combined with enzalutamide significantly suppressed cell growth (Fig.3E). The results were also confirmed

in C4–2B AKR1C3 cells (Fig.3F). These data suggest that AKR1C3 induced AR-V7 overexpression and thus confers resistance to enzalutamide treatment.

AKR1C3 controls AR/AR-V7 protein stabilization in resistant prostate cancer cells

To further dissect the underlying mechanisms of AKR1C3 mediated AR-V7 protein upregulation, we determined AR/AR-V7 protein stability in both C4–2B-neo and C4–2B-AKR1C3 cells. As shown in Fig.4A, overexpression of AKR1C3 significantly extended the half-life of AR-V7 protein in C4–2B-AKR1C3 cells (over 8 hours) compared to the control cells (less than 2 hours). AR-FL protein half-life was also extended in C4–2B-AKR1C3 cells. Next, we determined if AKR1C3 knockdown affected AR/AR-V7 protein stabilization in CWR22Rv1 cells. As shown in Fig.4B, AKR1C3 knockdown significantly shortened the half-life of AR-V7 protein (around 2 hours) in CWR22Rv1 cells compared to the vector transfected controls (> 8 hours). AR-FL protein half-life was also shortened by AKR1C3 knockdown in CWR22Rv1 cells. The results were also confirmed in C4–2B MDVR cells (Fig.4C). Previous studies showed that indomethacin is a potent AKR1C3 inhibitor that enhanced enzalutamide treatment by decreasing the testosterone level in resistant cells (11). Here we found indomethacin suppressed AR and AR variants expression in C4–2B MDVR cells (Fig.4D). Inhibiting proteasome activity by MG132 rescued AR/AR-V7 protein expression in C4–2B MDVR cells (Fig.4E). Additionally, indomethacin significantly enhanced AR/AR-V7 protein ubiquitination in C4–2B MDVR cells (Fig.4F). These data suggest that AKR1C3 stabilizes AR/AR-V7 protein levels through the ubiquitin-proteasome pathway.

Inhibition of AKR1C3 with indomethacin disrupts gene programs and suppresses AR/AR-V7 signaling in resistant cells

To further address the inhibitory effects of indomethacin in resistant prostate cancer cells, we analyzed the RNA sequencing data from C4–2B MDVR cells treated with indomethacin and identified gene programs that are regulated by AKR1C3 inhibition. Analyzing by GSEA, we identified that the unfolded protein response (UPR), p53 signaling, apoptosis and hypoxia pathways were the top pathways upregulated by indomethacin treatment. The pathways most down regulated include E2F targets, cell cycle and Myc targets (Fig.5A). Using hierarchical clustering to plot the heatmap with the genes found regulated by indomethacin, 4,941 genes were upregulated or down regulated by indomethacin (Fig.5B left). At the individual gene level, we determined that genes involved in UPR and ER stress (CHAC1, DDIT4, CEBPB and ATF6) and genes in the p53 and apoptosis pathways (TP53, CDKN1A and SOCS1) were upregulated in indomethacin treated cells. We also found that Myc and cell cycle pathway genes (Myc, MCM4 and CCNE2) and AR/AR-V7 regulated genes (KLK3, FKBP5, UBE2C) were down-regulated by indomethacin treatment (Fig.5B middle and right). Further GSEA revealed AR and AR-V7 pathways were significantly blocked by indomethacin treatment in C4–2B MDVR drug resistant cells (Fig.5C). The AR and AR-V7 target genes were verified by qRT-PCR. As shown in Fig.5D, KLK2, KLK3, NKX3–1, FKBP5, UBE2C and Myc were decreased by indomethacin treatment. Notably, AR-V7 preferentially regulated genes such as UBE2C and Myc were significantly suppressed by indomethacin treatment (Fig.5D). These results suggested indomethacin

treatment significantly disrupts the drug resistant gene programs and suppresses AR/AR-V7 signaling.

Orally administered indomethacin enhances enzalutamide treatment through AKR1C3/AR-V7 inhibition

Previous data suggested indomethacin enhanced enzalutamide treatment when administered through intraperitoneal (i.p.) injection (11). To further identify the potential activity of indomethacin *in vivo*, we determined its tumor inhibition effects though oral administration. As shown in Fig.6A–6C, CWR22Rv1 tumors were completely resistant to enzalutamide treatment, orally administered indomethacin significantly reduced tumor growth, and indomethacin combined with enzalutamide treatment further suppressed tumor growth. However, all treatment did not affect the mice body weight (Fig.6D). We also determined the intratumoral testosterone level of each group, as shown in Fig.6E, enzalutamide slightly decreased the testosterone level, however, indomethacin and indomethacin plus enzalutamide treatment group significantly decreased the tumor testosterone level. We also extracted tumor proteins and found that indomethacin alone and the combination treatment groups significantly decreased AR/AR-V7, c-Myc and Bcl-2 expression in these tumors. These results suggest that targeting AKR1C3 with small molecule indomethacin enhances enzalutamide treatment *in vivo* through suppressing both intratumoral testosterone and AR-V7 expression.

Discussion

Our study discovered a novel mechanism by which AKR1C3 activates the ubiquitin proteasome pathway and thus induces AR-V7 protein stabilization. We show that the AKR1C3 associated steroid hormone biosynthesis pathway is activated in enzalutamide resistant models. AR and AR-V7 signaling is reprogramed in resistant cells, possibly through AKR1C3 upregulation. We further determined that AKR1C3 promotes AR and AR-V7 stabilization in enzalutamide resistant cells. Targeting AKR1C3 with indomethacin significantly enhances enzalutamide treatment *in vivo* through inhibition of AR-V7. Our data highlight that AKR1C3 and AR-V7 are major contributors promoting prostate cancer resistance to ARSI. The main function of AKR1C3 is to catalyze the reduction of 5α-dihydrotestosterone to 5α-androstane-3α,17β-dior with its 3α-HSD activity and conversion of androstenedione to testosterone by its 17β-HSD activity (13). On the other hand, AKR1C3 also catalyzes the formation of prostaglandin (PG) $F_{2\alpha}$ and 11β-$PGF_{2\alpha}$ from PGH2 and PGD2, respectively. The $PGF_{2\alpha}$ and 11β-$PGF_{2\alpha}$ can inactivate peroxisome proliferator -activated receptor gamma (PPARγ) and has anti-proliferative effects (24). Emerging evidence show that AKR1C3 not only functions as an enzyme, but also plays important roles in regulating oncogenic protein expression and activity. Several AKR1C3 oncogenic regulators have been identified previously. ERG upregulates AKR1C3 expression and leads to biochemical reduction of 5α-Androstanedione to DHT in prostate cancer cells (25). AKR1C3 also regulates E3 ligase SIAH2 protein stability and thus enhances SIAH2-dependent AR activity in prostate cancer cells (26). In the present study, we found that AKR1C3 involved steroidgenesis pathway plays a central role in enzalutamide resistance. Two independent databases both indicated that androgen biosynthesis pathway was activated

in enzalutamide resistant cells and xenograft tumors. Additionally, we discover a new function of AKR1C3 that AKR1C3 promotes AR-V7 stabilization at the protein level. Our findings highlight the importance of AKR1C3 in next generation anti-androgen resistance. Targeting AKR1C3 with indomethacin leads to AR/AR-V7 degradation and may be a valid strategy to overcome the resistance.

As a non-steroidal anti-inflammatory drug (NSAID), indomethacin is used for reducing pain and inflammation by inhibiting COX-2. Emerging evidence suggests that indomethacin inhibits AKR1C3 activity and enhances ARSI treatments (11, 12). Indomethacin significantly promotes AR/AR-V7 protein degradation through activation of the ubiquitin proteasome system and affects the stability of other proteins as well. Currently, the clinical trial of indomethacin and enzalutamide combination treatment in CRPC patients is ongoing () (27). Our study provides further support that targeting AKR1C3 by indomethacin significantly improves enzalutamide treatment through AR/AR-V7 inhibition. The second generation ARSI brought a new revolution to advanced prostate cancer therapy. Unfortunately, the initial responders will inevitably develop resistance. AR variants which lack the ligand-binding domain (LBD), particularly AR-V7, are involved in resistance to ARSI. They are frequently expressed in CRPC patients and correlates with poor survival (28, 29). These variants constitutively activate AR target genes and promote the androgen/AR transcriptional pathway in the absence of ligand. We previously reported that C4–2B cells treated chronically with enzalutamide (C4–2B MDVR) had significantly enhanced AR-variants expression, which suggested AR variants mediated distinct AR activation is sufficient to support cell proliferation and drug resistance (30). AR deregulation has been found in 80% CRPC patients (31). AR overexpression in prostate cancer cells confers AR hypersensitivity to low levels of androgen and might result the drug resistance (32). In this study, we found that upregulation of AR expression induced by androgen treatment was more profound in enzalutamide resistant cells than parental cells. Bioinformatic analysis revealed that AR was deregulated and distinct AR pathway was reactivated in C4–2B MDVR cells. Several AR co-activators, such as FHL2, MED12, FKBP4 and NCOA3, were up regulated. Notably, FHL2 was defined not only as a new AR co-regulator but also bound with AR variants especially AR-V7 in prostate cancer cells. Nuclear localization of FHL2 in CRPC cells may promote constitutive AR-V7 activation (33). Our data suggested that chronic enzalutamide treatment in prostate cancer cells deregulated AR/AR-V7 signaling in C4–2B MDVR cells, possibly through the AKR1C3 mediated steroid hormone biosynthesis pathway activation.

Previous studies established that AR variants are generated through structure rearrangement of AR gene or RNA splicing. AR-V7 can be regulated by various modulators of RNA splicing, such as U2AF65, ASF/SF2 (8) and JMJD1A (34). It can also be regulated through cistromes, such as Hoxb13 (35) and FOXA1 (36). However, mechanisms of AR variant protein regulation have not yet been fully investigated. We recently reported that HSP70/STUB1complex mediated AR-V7 protein homeostasis controls next generation anti-androgen resistance. HSP70 binds AR-V7 and forms a complex assisting AR-V7 protein maturation. STUB1 induces AR-V7 protein degradation by blocking HSP70/AR-V7 complex formation (37). Li et al. reported that PP-1 and Akt signaling regulates AR-V7 phosphorylation on serine 213 through E3 ligase MDM2. MDM2 recognizes the AR-V7

phosphorylation site and induces AR-V7 ubiquitination and protein degradation (38). A previous study found that AKR1C3 is an AR co-activator that interacts with AR in prostate cancer cells, xenograft tumor samples and CRPC patient samples (18). Our data demonstrating that AKR1C3 interacts with AR-V7 reinforces the novel function of AKR1C3. AKR1C3 not only controls the full length AR required activation via ligand-binding but also regulates the truncated AR that bypasses this activation. Our data indicated that targeting AKR1C3 by shRNA or the small molecule inhibitor indomethacin significantly suppressed AR-V7 protein expression through the ubiquitin proteasome pathway alteration. Notably, c-Myc and Bcl-2 which are oncogenic proteins possibly regulated by AR-V7 were also suppressed by AKR1C3 inhibition. Myc can deregulate the AR transcriptional program and drive prostate cancer progression (39, 40). Our data suggest that AKR1C3 plays an important role in controlling androgen signaling and prostate cancer progression.

Collectively, our results identify a new role for AKR1C3 in next generation anti-androgen resistance. We demonstrated that the AKR1C3/AR-V7 complex collaboratively confers resistance to AR-targeted therapies. Targeting AKR1C3 not only can inhibit intracrine androgen synthesis, but also can further suppress AR/AR-V7 signaling by altering its protein stability.

Supplementary Material

Refer to Web version on PubMed Central for supplementary material.

Acknowledgments

We sincerely thank the Dr. Clifford G. Tepper and Genomics Shared Resource (GSR) at the UC Davis Comprehensive Cancer Center for their assistance in our study. This work was supported in part by grants NIH/NCI CA168601, CA179970, DOD PC150229, and the U.S. Department of Veterans Affairs, Office of Research & Development BL&D grant number I01BX0002653 (A.C.G), a Research Career Scientist Award (A.C.G). A.C.G is also a Research Career Scientist at VA Northern California Health Care System, Mather, California.

Financial Support: This work is part by grants NIH/NCI CA168601 (A.C. G), CA179970 (A.C. G), DOD PC150229 (A.C. G), and the U.S. Department of Veterans Affairs, Office of Research & Development BL&D grant number I01BX0002653 (A.C. G),

References

1. Scher HI, Fizazi K, Saad F, Taplin ME, Sternberg CN, Miller K, et al. Increased survival with enzalutamide in prostate cancer after chemotherapy. The New England journal of medicine. 2012;367:1187–97. [PubMed: 22894553]
2. de Bono JS, Logothetis CJ, Molina A, Fizazi K, North S, Chu L, et al. Abiraterone and increased survival in metastatic prostate cancer. The New England journal of medicine. 2011;364:1995–2005. [PubMed: 21612468]
3. Smith MR, Saad F, Chowdhury S, Oudard S, Hadaschik BA, Graff JN, et al. Apalutamide Treatment and Metastasis-free Survival in Prostate Cancer. The New England journal of medicine. 2018;378:1408–18. [PubMed: 29420164]
4. Cook T, Sheridan WP. Development of GnRH antagonists for prostate cancer: new approaches to treatment. The oncologist. 2000;5:162–8. [PubMed: 10794807]
5. Antonarakis ES, Lu C, Wang H, Luber B, Nakazawa M, Roeser JC, et al. AR-V7 and resistance to enzalutamide and abiraterone in prostate cancer. The New England journal of medicine. 2014;371:1028–38. [PubMed: 25184630]

6. Hu R, Lu C, Mostaghel EA, Yegnasubramanian S, Gurel M, Tannahill C, et al. Distinct transcriptional programs mediated by the ligand-dependent full-length androgen receptor and its splice variants in castration-resistant prostate cancer. Cancer Res. 2012;72:3457–62. [PubMed: 22710436]
7. Kohli M, Ho Y, Hillman DW, Van Etten JL, Henzler C, Yang R, et al. Androgen Receptor Variant AR-V9 Is Coexpressed with AR-V7 in Prostate Cancer Metastases and Predicts Abiraterone Resistance. Clinical cancer research : an official journal of the American Association for Cancer Research. 2017;23:4704–15.
8. Liu LL, Xie N, Sun S, Plymate S, Mostaghel E, Dong X. Mechanisms of the androgen receptor splicing in prostate cancer cells. Oncogene. 2014;33:3140–50. [PubMed: 23851510]
9. Nyquist MD, Li Y, Hwang TH, Manlove LS, Vessella RL, Silverstein KA, et al. TALEN-engineered AR gene rearrangements reveal endocrine uncoupling of androgen receptor in prostate cancer. Proceedings of the National Academy of Sciences of the United States of America. 2013;110:17492–7. [PubMed: 24101480]
10. Li Y, Alsagabi M, Fan D, Bova GS, Tewfik AH, Dehm SM. Intragenic rearrangement and altered RNA splicing of the androgen receptor in a cell-based model of prostate cancer progression. Cancer Res. 2011;71:2108–17. [PubMed: 21248069]
11. Liu C, Lou W, Zhu Y, Yang JC, Nadiminty N, Gaikwad NW, et al. Intracrine Androgens and AKR1C3 Activation Confer Resistance to Enzalutamide in Prostate Cancer. Cancer research. 2015;75:1413–22. [PubMed: 25649766]
12. Liu C, Armstrong CM, Lou W, Lombard A, Evans CP, Gao AC. Inhibition of AKR1C3 Activation Overcomes Resistance to Abiraterone in Advanced Prostate Cancer. Molecular cancer therapeutics. 2017;16:35–44. [PubMed: 27794047]
13. Stanbrough M, Bubley GJ, Ross K, Golub TR, Rubin MA, Penning TM, et al. Increased expression of genes converting adrenal androgens to testosterone in androgen-independent prostate cancer. Cancer research. 2006;66:2815–25. [PubMed: 16510604]
14. Wako K, Kawasaki T, Yamana K, Suzuki K, Jiang S, Umezu H, et al. Expression of androgen receptor through androgen-converting enzymes is associated with biological aggressiveness in prostate cancer. Journal of clinical pathology. 2008;61:448–54. [PubMed: 17720776]
15. Adeniji AO, Chen M, Penning TM. AKR1C3 as a target in castrate resistant prostate cancer. The Journal of steroid biochemistry and molecular biology. 2013;137:136–49. [PubMed: 23748150]
16. Labrie F, Luu-The V, Lin SX, Labrie C, Simard J, Breton R, et al. The key role of 17 beta-hydroxysteroid dehydrogenases in sex steroid biology. Steroids. 1997;62:148–58. [PubMed: 9029730]
17. Bauman DR, Steckelbroeck S, Williams MV, Peehl DM, Penning TM. Identification of the major oxidative 3alpha-hydroxysteroid dehydrogenase in human prostate that converts 5alpha-androstane-3alpha,17beta-diol to 5alpha-dihydrotestosterone: a potential therapeutic target for androgen-dependent disease. Molecular endocrinology. 2006;20:444–58. [PubMed: 16179381]
18. Yepuru M, Wu Z, Kulkarni A, Yin F, Barrett CM, Kim J, et al. Steroidogenic enzyme AKR1C3 is a novel androgen receptor-selective coactivator that promotes prostate cancer growth. Clinical cancer research : an official journal of the American Association for Cancer Research. 2013;19:5613–25.
19. Liu C, Lou W, Zhu Y, Nadiminty N, Schwartz CT, Evans CP, et al. Niclosamide inhibits androgen receptor variants expression and overcomes enzalutamide resistance in castration-resistant prostate cancer. Clinical cancer research : an official journal of the American Association for Cancer Research. 2014;20:3198–210.
20. Liu C, Armstrong CM, Lou W, Lombard AP, Cucchiara V, Gu X, et al. Niclosamide and Bicalutamide Combination Treatment Overcomes Enzalutamide- and Bicalutamide-Resistant Prostate Cancer. Molecular cancer therapeutics. 2017;16:1521–30. [PubMed: 28500234]
21. Subramanian A, Tamayo P, Mootha VK, Mukherjee S, Ebert BL, Gillette MA, et al. Gene set enrichment analysis: a knowledge-based approach for interpreting genome-wide expression profiles. Proceedings of the National Academy of Sciences of the United States of America. 2005;102:15545–50. [PubMed: 16199517]

22. Gaikwad NW. Ultra performance liquid chromatography-tandem mass spectrometry method for profiling of steroid metabolome in human tissue. Analytical chemistry. 2013;85:4951–60. [PubMed: 23597399]

23. Arora VK, Schenkein E, Murali R, Subudhi SK, Wongvipat J, Balbas MD, et al. Glucocorticoid receptor confers resistance to antiandrogens by bypassing androgen receptor blockade. Cell 2013;155:1309–22. [PubMed: 24315100]

24. Desmond JC, Mountford JC, Drayson MT, Walker EA, Hewison M, Ride JP, et al. The aldo-keto reductase AKR1C3 is a novel suppressor of cell differentiation that provides a plausible target for the non-cyclooxygenase-dependent antineoplastic actions of nonsteroidal anti-inflammatory drugs. Cancer research. 2003;63:505–12. [PubMed: 12543809]

25. Powell K, Semaan L, Conley-LaComb MK, Asangani I, Wu YM, Ginsburg KB, et al. ERG/AKR1C3/AR Constitutes a Feed-Forward Loop for AR Signaling in Prostate Cancer Cells. Clinical cancer research : an official journal of the American Association for Cancer Research. 2015;21:2569–79. [PubMed: 25754347]

26. Fan L, Peng G, Hussain A, Fazli L, Guns E, Gleave M, et al. The Steroidogenic Enzyme AKR1C3 Regulates Stability of the Ubiquitin Ligase Siah2 in Prostate Cancer Cells. The Journal of biological chemistry. 2015;290:20865–79. [PubMed: 26160177]

27. Pan PL Chong-xian, Evans Christopher P., Parikh Mamta, de Vere White Ralph, Marc Dall'era, Chengfei Liu, Robles Daniel, Gao Allen A phase Ib/II trial of indomethacin and enzalutamide to treat castration-resistant prostate cancer (CRPC). Journal Of Clinical Oncology. 2018;36, no. 6_suppl.

28. Dehm SM, Schmidt LJ, Heemers HV, Vessella RL, Tindall DJ. Splicing of a novel androgen receptor exon generates a constitutively active androgen receptor that mediates prostate cancer therapy resistance. Cancer Res. 2008;68:5469–77. [PubMed: 18593950]

29. Hu R, Dunn TA, Wei S, Isharwal S, Veltri RW, Humphreys E, et al. Ligand-independent androgen receptor variants derived from splicing of cryptic exons signify hormone-refractory prostate cancer. Cancer research. 2009;69:16–22. [PubMed: 19117982]

30. Liu C, Lou W, Zhu Y, Nadiminty N, Schwartz C, Evans CP, et al. Niclosamide inhibits androgen receptor variants expression and overcomes Enzalutamide resistance in castration resistant prostate cancer. Clinical cancer research : an official journal of the American Association for Cancer Research. 2014.

31. Linja MJ, Savinainen KJ, Saramaki OR, Tammela TL, Vessella RL, Visakorpi T. Amplification and overexpression of androgen receptor gene in hormone-refractory prostate cancer. Cancer research. 2001;61:3550–5. [PubMed: 11325816]

32. Waltering KK, Helenius MA, Sahu B, Manni V, Linja MJ, Janne OA, et al. Increased expression of androgen receptor sensitizes prostate cancer cells to low levels of androgens. Cancer research. 2009;69:8141–9. [PubMed: 19808968]

33. McGrath MJ, Binge LC, Sriratana A, Wang H, Robinson PA, Pook D, et al. Regulation of the transcriptional coactivator FHL2 licenses activation of the androgen receptor in castrate-resistant prostate cancer. Cancer research. 2013;73:5066–79. [PubMed: 23801747]

34. Fan L, Zhang F, Xu S, Cui X, Hussain A, Fazli L, et al. Histone demethylase JMJD1A promotes alternative splicing of AR variant 7 (AR-V7) in prostate cancer cells. Proceedings of the National Academy of Sciences of the United States of America. 2018;115:E4584–E93. [PubMed: 29712835]

35. Chen Z, Wu D, Thomas-Ahner JM, Lu C, Zhao P, Zhang Q, et al. Diverse AR-V7 cistromes in castration-resistant prostate cancer are governed by HoxB13. Proceedings of the National Academy of Sciences of the United States of America. 2018.

36. Jones D, Wade M, Nakjang S, Chaytor L, Grey J, Robson CN, et al. FOXA1 regulates androgen receptor variant activity in models of castrate-resistant prostate cancer. Oncotarget. 2015;6:29782–94. [PubMed: 26336819]

37. Liu C, Lou W, Yang JC, Liu L, Armstrong CM, Lombard AP, et al. Proteostasis by STUB1/HSP70 complex controls sensitivity to androgen receptor targeted therapy in advanced prostate cancer. Nature communications. 2018;9:4700.

38. Li Y, Xie N, Gleave ME, Rennie PS, Dong X. AR-v7 protein expression is regulated by protein kinase and phosphatase. Oncotarget 2015;6:33743–54. [PubMed: 26378044]

39. Barfeld SJ, Urbanucci A, Itkonen HM, Fazli L, Hicks JL, Thiede B, et al. c-Myc Antagonises the Transcriptional Activity of the Androgen Receptor in Prostate Cancer Affecting Key Gene Networks. EBioMedicine. 2017;18:83–93. [PubMed: 28412251]

40. Bai S, Cao S, Jin L, Kobelski M, Schouest B, Wang X, et al. A positive role of c-Myc in regulating androgen receptor and its splice variants in prostate cancer. Oncogene. 2019.

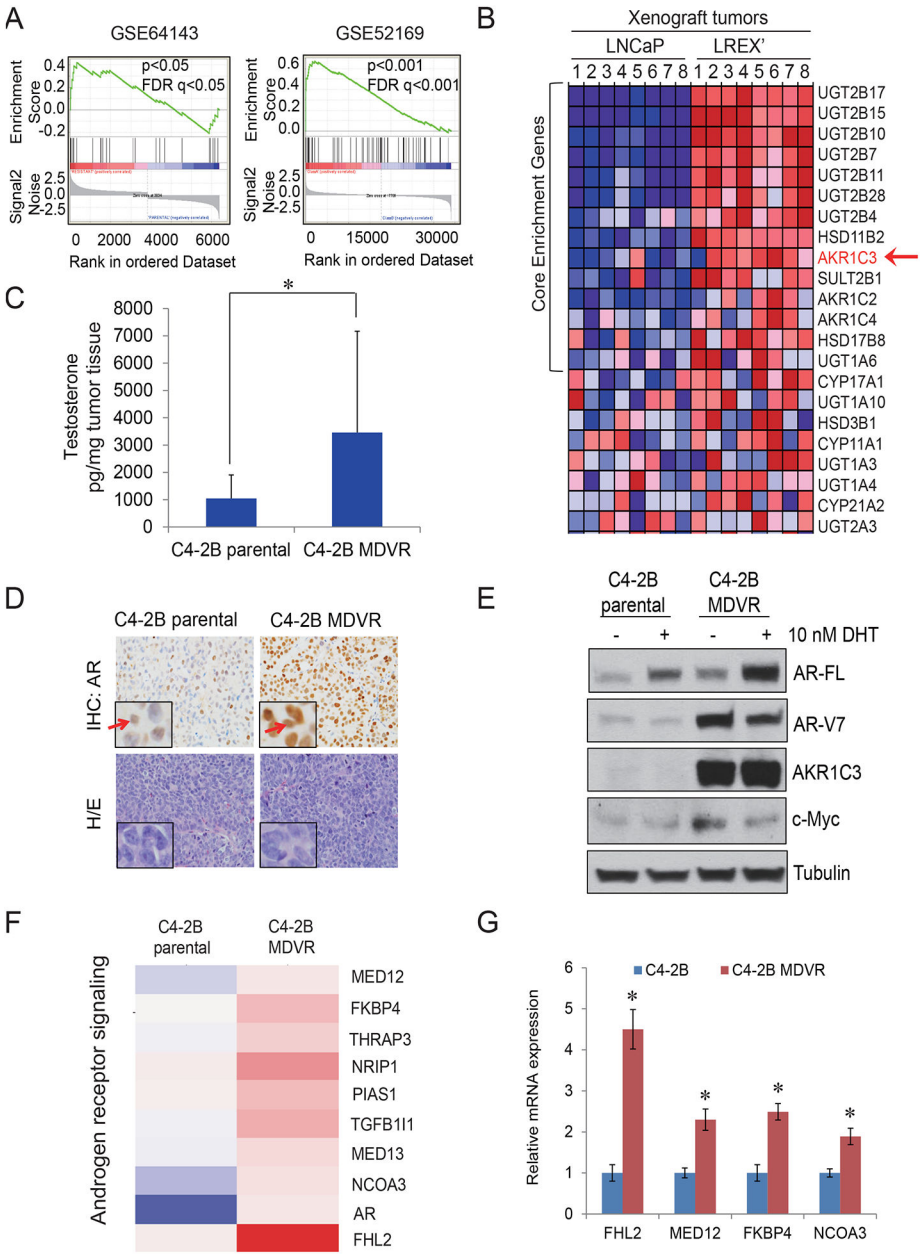

Figure 1. AR/AR-V7 signaling is reprogramed in C4-2B MDVR cells through AKR1C3 up regulation.

A. The steroid Hormone Biosynthesis pathway in two independent enzalutamide resistant models was analyzed by GSEA. GSE64143 is the microarray data set from C4–2B parental and C4–2B MDVR cells. GSE52619 is the mouse LNCaP/AR xenograft tumors derived from Enza resistant LREX' cells compared with LNCaP xenograft tumors. B. Heatmap of Enza resistant xenograft tumors. C. C4–2B parental and C4–2B MDVR xenograft tumors were processed and the testosterone level was determined by LC-MS. D. AR staining was determined by IHC from C4–2B parental tumor and C4–2B MDVR tumor. E. C4–2B parental and C4–2B MDVR cells were cultured in CS-FBS condition and treated with 10nM DHT for 3 days, whole cell lysates was collected and subjected to western blot. F.

Expression of transcripts encoding for androgen receptor signaling was analyzed. Genes that were regulated 1.3 fold between C4–2B parental cells and C4–2B MDVR cells were enriched and heat map was generated by Subio platform. G. Total RNA from C4–2B parental and C4–2B MDVR cells was extracted and the mRNA levels of FHL2, MED12, FKBP4 and NCOA3 were determined by qRT-PCR. AR-FL, AR-V7, AKR1C3, c-Myc were determined, tubulin was set up as control. * $p<0.05$

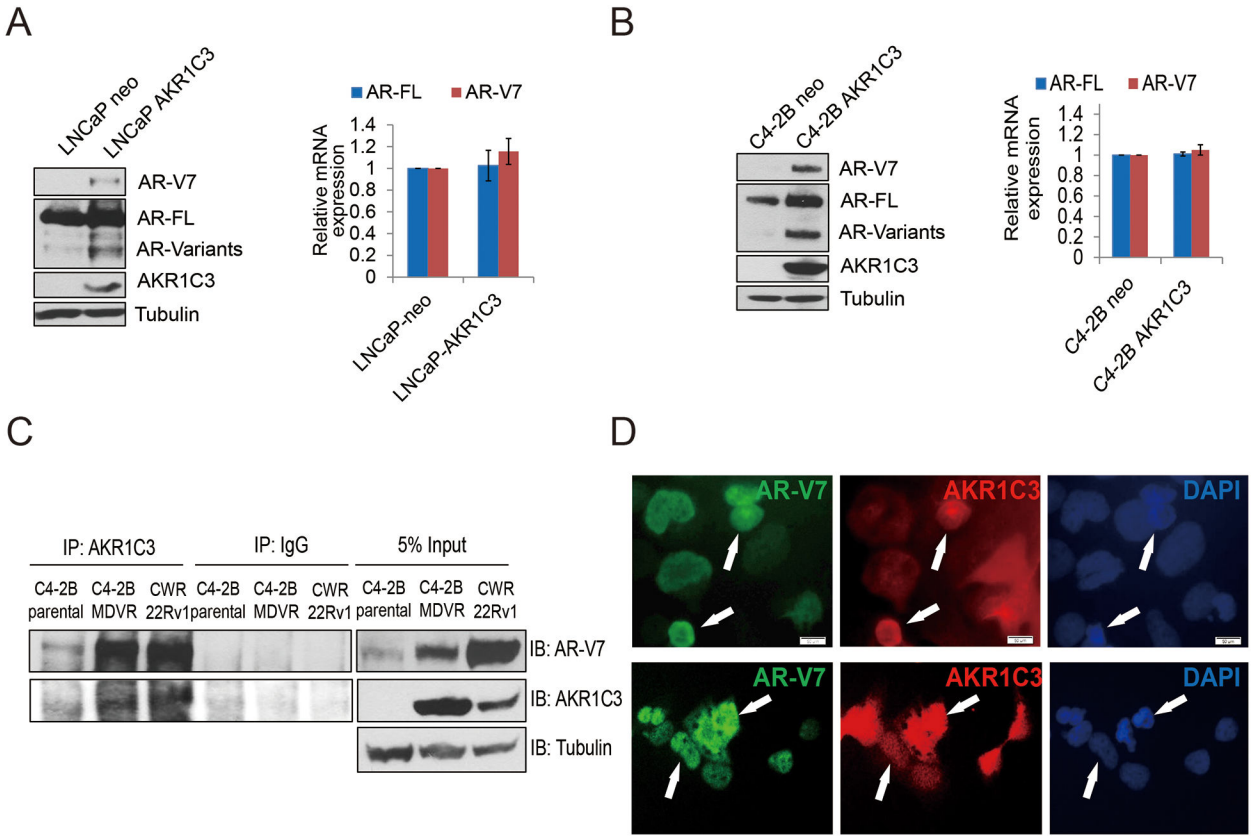

Figure 2. AKR1C3 induces AR/AR-V7 protein expression.

A. LNCaP-neo and LNCaP-AKR1C3 were cultured in FBS conditions for 5–7 days, whole cell lysates were harvested and subjected to western blot. AR-V7, AR-FL, and AKR1C3 expression was determined and tubulin was used as internal control. Total RNA was extracted and the mRNA levels of AR, AR-V7 and AKR1C3 were determined by qRT-PCR. B. C4–2B-neo and C4–2B-AKR1C3 cells were cultured in FBS conditions for 5–7 days, whole cell lysates were harvested and subjected to western blot. AR-V7, AR-FL, and AKR1C3 expression was determined and tubulin was used as internal control. Total RNA was extracted and the mRNA levels of AR, AR-V7 and AKR1C3 were determined by qRT-PCR. C. C4–2B, C4–2B MDVR and CWR22Rv1 cells were cultured in FBS condition and whole cell lysates were immunopreciptated with anti-AKR1C3 antibody and blotted with indicated antibodies. D. 293 cells were co-transfected with AR-V7, and AKR1C3 for 3 days, AR-V7 and AKR1C3 were visualized by dual immunofluorescence staining. White arrows indicated the typical staining cells in each group.

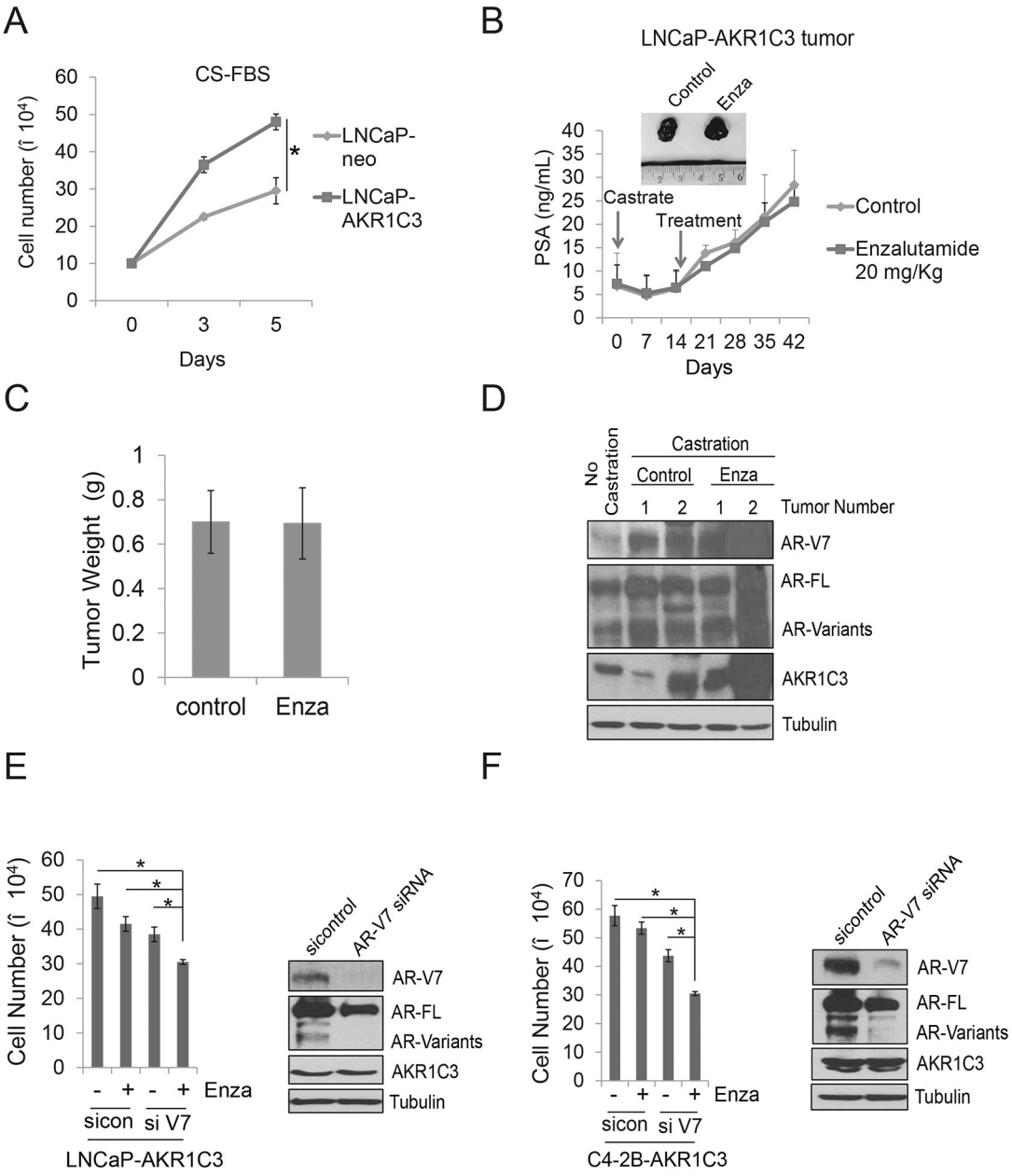

Figure 3. AKR1C3 promotes enzalutamide resistance through AR-V7.

A. LNCaP-neo and LNCaP-AKR1C3 cells were cultured in CS-FBS condition, total cell numbers were determined on 3 and 5 days. B. The orthotopically injected LNCaP-AKR1C3 tumor growth curve reflected by mouse serum PSA. The castrated relapsed LNCaP-AKR1C3 tumors were treated with vehicle control or 20mg/Kg enzalutamide for 4 weeks (n=4). Serum PSA level was monitored by PSA ELISA. C. The tumor weight was determined in control and enzalutamide treated groups. D. The LNCaP-AKR1C3 tumors were processed, whole tumor lysates were collected and subjected to western blot. AR-V7, AR-FL and AKR1C3 expression was determined. E-F. AR-V7 was knocked down in LNCaP-AKR1C3 and C4–2B-AKR1C3 cells by AR-V7 siRNA, cells were then treated with 20 μM enzalutamide for 5 days and total cell number was determined and whole cell lysates

were collected and the knockdown effects were determined by western blot. Enza: Enzalutamide * $p<0.05$.

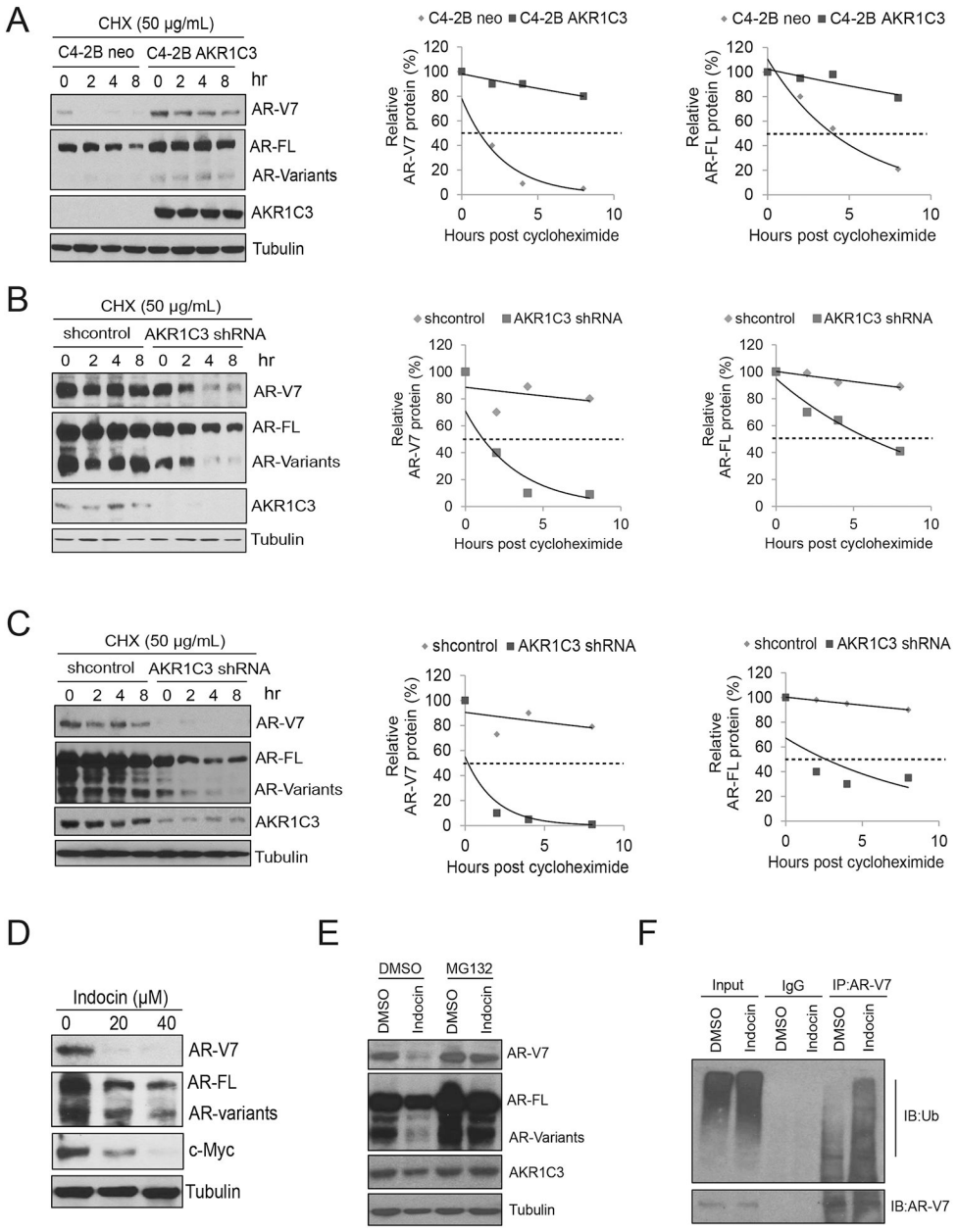

Figure 4. AKR1C3 controls AR/AR-V7 protein stabilization in resistant prostate cancer.

A. C4–2B neo and C4–2B AKR1C3 cells were treated with 50 μg cycloheximide. Whole cell lysates were collected at 0, 2, 4 and 8 hours after treatment and subjected to western blot. Half-lives of AR-V7 and AR-FL were calculated. B. CWR22Rv1 cells were infected with lenti-vector or lenti-shAKR1C3 particles for 48 hours and then treated with 50 μg cycloheximide. Whole cell lysates were collected at 0, 2, 4 and 8 hours after treatment and subjected to western blot. Half-lives of AR-V7 and AR-FL were calculated. C. C4–2B MDVR cells were infected with lenti-vector or lenti-shAKR1C3 particles for 48 hours and then treated with 50 μg cycloheximide. Whole cell lysates were collected at 0, 2, 4 and 8 hours after treatment and subjected to western blot. Half-lives of AR-V7 and AR-FL were calculated. D. C4–2B MDVR cells were treated with different doses of indomethacin for 3

days. Whole cell lysates were collected and subjected to western blot. E. C4–2B MDVR cells were treated with indomethacin for 3 days and then treated with 5 μg/mL MG132 for additional 6 hours. Whole cell lysates were collected and subjected to western blot. F. C4–2B MDVR cells were treated with indomethacin for 3 days, then treated with or without 5μM MG132 for additional 6 hours. Whole cell lysates were collected and immunopreciptated with AR-V7 antibody and blotted with anti-Ub and AR-V7 antibodies. Indocin: Indomethacin.

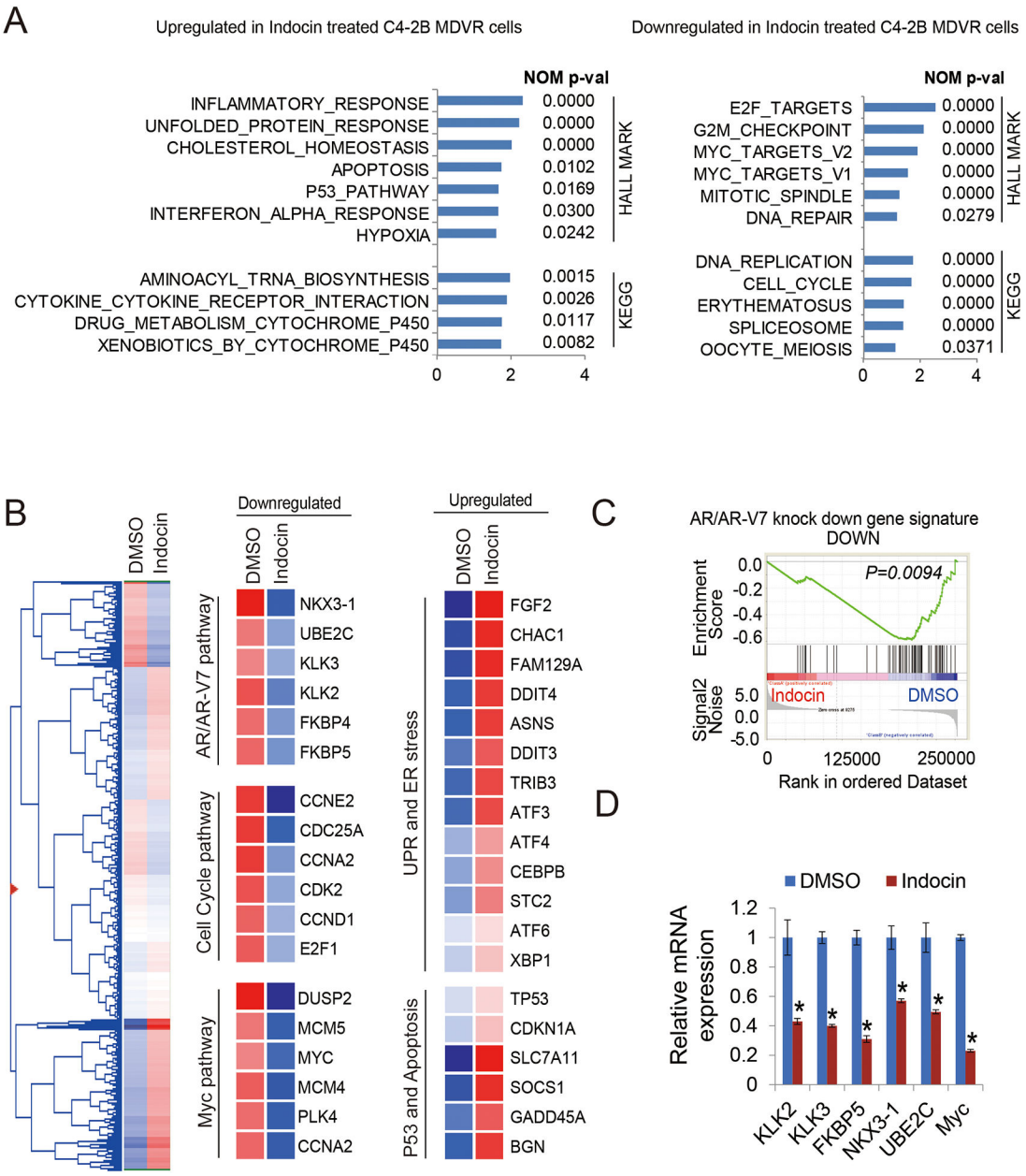

Figure 5. Inhibition of AKR1C3 with indomethacin down regulates Myc pathway and AR/AR-V7 signaling in resistant cells.

A. GSEA of top enriched gene sets in C4–2B MDVR cells treated with indomethacin. The upregulated and down regulated gene sets from the Hallmark and KEGG platforms were output by GSEA. B. Heatmap and hierarchical clustering of the differentially expressed genes (DEGs) with indomethacin treatment in C4–2B MDVR cells with FC > 1.2, as compared to vehicle (DMSO). The genes are displayed in rows and the normalized counts per sample are displayed in columns. Red indicates up-regulated and blue designates down-regulated expression levels. Middle and right, Cell cycle, Myc, UPR and ER stress, P53 and apoptosis, AR and AR-V7 activity-signature genes that were altered in expression are displayed, C. GSEA of the AR and AR-V7 gene signatures in C4–2B MDVR cells treated

with HSP70 inhibitors (right). The signature was defined by genes that underwent significant expression changes as a result of AR and AR-V7 knockdown in PCa cells. D. qRT-PCR analysis of the indicated genes in C4–2B MDVR cells treated with DMSO or with indomethacin for 3 days. Indocin: Indomethacin. * $p<0.05$.

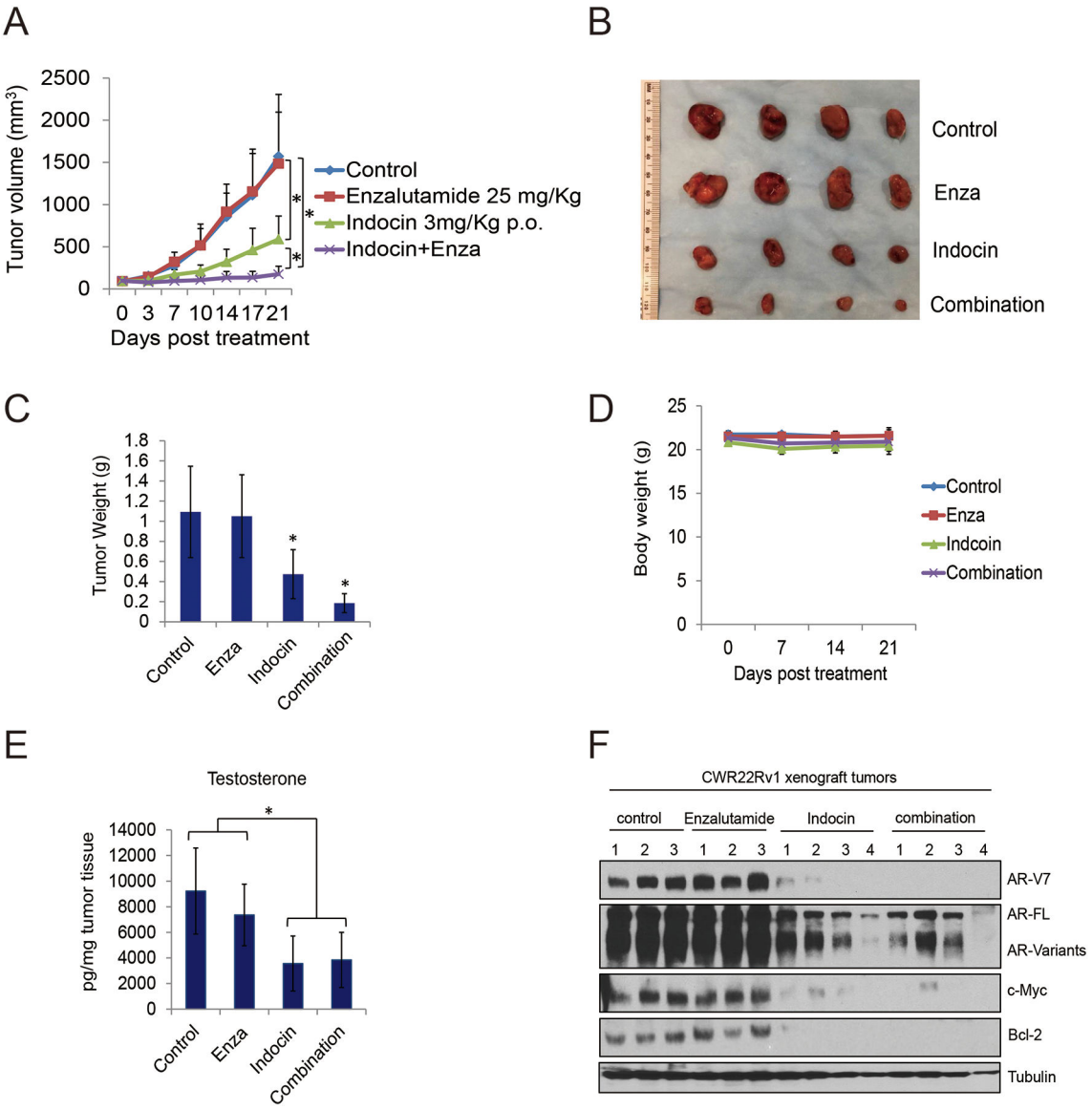

Figure 6. Orally administrated indomethacin enhanced enzalutamide treatment in vivo.

A-B. Mice bearing CWR22Rv1 xenografts were treated with vehicle control, enzalutamide (25 mg/Kg p.o), indomethacin (3mg/Kg p.o.) or their combination for 3 weeks. Tumor volumes were measured twice weekly and the tumors were collected. C. The tumors were weighted in each group. D. Mice body weight was determined every week in each group. E. the tumors were processed and the intratumoral testosterone level was determined by LC-MS. F. Total tumor lysates in each group were collected. AR-V7, AR-FL, c-Myc, Bcl-2 and Tubulin were subjected to western blot. Enza: Enzalutamide. Indocin: Indomethacin. * $p<0.05$.